Thermo-Kinetic Model of Burning

May 2008

DOT/FAA/AR-TN08/17

This document is available to the U.S. public through the National Technical Information Services (NTIS), Springfield, Virginia 22161.

U.S. Department of Transportation
Federal Aviation Administration

NOTICE

This document is disseminated under the sponsorship of the U.S. Department of Transportation in the interest of information exchange. The United States Government assumes no liability for the contents or use thereof. The United States Government does not endorse products or manufacturers. Trade or manufacturer's names appear herein solely because they are considered essential to the objective of this report. This document does not constitute FAA certification policy. Consult your local FAA aircraft certification office as to its use.

This report is available at the Federal Aviation Administration William J. Hughes Technical Center's Full-Text Technical Reports page: actlibrary.act.faa.gov in Adobe Acrobat portable document format (PDF).

1. Report No. DOT/FAA/AR-TN08/17	2. Government Accession No.	3. Recipient's Catalog No.
4. Title and Subtitle THERMO-KINETIC MODEL OF BURNING		5. Report Date May 2008
		6. Performing Organization Code
7. Author(s) Stanislav I. Stoliarov* and Richard E. Lyon		8. **Performing Organization Report No.**
9. Performing Organization Name and Address *SRA International, Inc. 3120 Fire Road Egg Harbor Township, NJ 08234 Federal Aviation Administration William J. Hughes Technical Center Airport and Aircraft Safety Research and Development Division Atlantic City International Airport, NJ 08405		10. Work Unit No. (TRAIS)
		11. Contract or Grant No.
12. Sponsoring Agency Name and Address U.S. Department of Transportation Federal Aviation Administration Air Traffic Organization Operations Planning Office of Aviation Research and Development Washington, DC 20591		13. Type of Report and Period Covered Technical Note
		14. Sponsoring Agency Code ANM-115
15. Supplementary Notes		

16. Abstract

One main obstacle in developing more effective passive fire protection for transportation is the lack of a quantitative understanding of the relations between the results of various materials fire tests used in this field. The need for multiple testing techniques arises from the complexity of fire phenomena and their sensitivity to environmental conditions. This study addressed this problem by developing a computational tool that predicts the behavior of materials exposed to fire. While it is not expected that this tool will eliminate the need for fire testing, the goal is to considerably reduce the number and complexity of the tests necessary for a comprehensive characterization of the materials of interest. The foundation of this tool is a mathematical model that describes transient thermal energy transport, chemical reactions, and the transport of gases through the condensed phase. The model also captures important aspects of a material's behavior such as charring and intumescence. This technical note provides a detailed description of the one-dimensional version of this model and summarizes the results of the model's verification.

17. Key Words Pyrolysis, Combustion, Polymer, Model	18. Distribution Statement This document is available to the U.S. public through the National Technical Information Service, Springfield, VA 22161.		
19. Security Classif. (of this report) Unclassified	20. Security Classif. (of this page) Unclassified	21. No. of Pages 32	22. Price

Form DOT F 1700.7 (8-72)   Reproduction of completed page authorized

TABLE OF CONTENTS

LIST OF FIGURES

LIST OF SYMBOLS

T	Temperature
c	Heat capacity
m	Mass
V	Volume
ρ	Density
γ	Swelling factor
θ	Stoichiometric coefficient
h	Heat of reaction
r	Rate of reaction
q	Rate of heat transfer
k	Thermal conductivity (when not used as a subscript)
S	Surface area
j	Rate of mass transfer (when not used as a subscript)
λ	Gas transfer coefficient
P	Pressure
t	Time
v	Convection coefficient
ε	Emissivity
f	Radiative heat flux
a	Absorbance
α	Absorption coefficient
Φ	Energy density

EXECUTIVE SUMMARY

One main obstacle in developing more effective passive fire protection for transportation is the lack of a quantitative understanding of the relations between the results of various materials fire tests used in this field. The need for multiple testing techniques arises from the complexity of fire phenomena and their sensitivity to environmental conditions. Many applications for which fire safety is a concern require development of a new test that mimics the most probable fire scenario. With few exceptions, these tests are expensive to build and operate. They also usually require a significant amount of material.

This study addressed this problem by developing a computational tool that predicts the behavior of materials under fire conditions. While it is not expected that this tool will eliminate the need for fire testing, it should be able to considerably reduce the number and complexity of the tests necessary for a comprehensive characterization of the materials of interest. The foundation of this tool is a mathematical model that describes transient thermal energy transport, chemical reactions, and the transport of gases through the condensed phase. The model also captures important aspects of a material's behavior such as charring and intumescence. This technical note provides a detailed description of the one-dimensional version of this model and summarizes the results of the model's verification.

INTRODUCTION

A substantial number of studies have been dedicated to the development of mathematical models that describe degradation of solid materials exposed to external heat flux. These models range in their complexity from analytical formulations based on assumption of a steady state [1 and 2] to complete, numerical solutions of the transient heat and mass transport coupled with chemical reactions [3 and 4]. Most of these models are one-dimensional. They predict the rate of mass loss from a unit area of the exposed surface. Some models incorporate a description of the gas phase combustion. Such models, which are usually two-dimensional, are frequently used to simulate the spread of flame [5 and 6]. Potentially, all of these models can be employed to understand and predict materials flammability. However, their utilization has been hampered by reliance on assumptions that make each of them applicable to a relatively narrow range of conditions and limited number of materials.

The purpose of this study was to develop a versatile computational tool capable of modeling pyrolysis and combustion of a wide range of materials including composites. This approach is called a thermo-kinetic model, or ThermaKin, because it combines transient thermal energy transport and material transformations described by means of chemical kinetics. The model includes a description of the transport of gases through the condensed phase and tracks changes in the volume of material. The complexity of the model can be manipulated by introducing or removing material components, which are characterized by temperature-dependent physical and chemical properties. At this stage, the one-dimensional version of this model has been completed. This version simulates conditions encountered in bench-scale fire calorimeters [7 and 8]. It is equipped with flexible boundary conditions that include time-dependent radiative and convective heat fluxes and possible in-depth absorption of the radiation. Surface ignition is simulated by altering the heat fluxes when a specified mass flux of decomposition products is reached. At the next stage of development, this model will be expanded to include a two-dimensional simulator of flame spread.

MODEL DESCRIPTION

COMPONENTS AND REACTIONS.

In ThermaKin, material is represented by a mixture of components. Every component is characterized by density, heat capacity, thermal conductivity, gas transfer coefficient, emissivity, and absorption coefficient. The first four properties in this list are defined by a flexible function of temperature (T),

$$\text{property} = p_0 + p_1 T + p_n T^n \tag{1}$$

where p_0, p_1, p_n, and n are user-specified parameters. Emissivity and absorption coefficients are defined by constants. All components are divided into three categories: solids, liquids, and gases. This categorization is used in the calculation of the volume of material, as explained below.

1

The heat capacity (c) of a given amount of material is calculated as

$$c = \sum_{i=1}^{N_c} m_i c_i \tag{2}$$

where m_i and c_i are mass and heat capacity of the i-th component; and N_c is the number of components. The volume of material (V) is defined by

$$V = \sum_{s=1}^{N_s} \frac{m_s}{\rho_s} + \sum_{l=1}^{N_l} \frac{m_l}{\rho_l} + \gamma \sum_{g=1}^{N_g} \frac{m_g}{\rho_g} \tag{3}$$

where ρ is component density. Subscripts s, l, and g are used to refer to solid, liquid, and gaseous components, respectively. Swelling factor γ, which may assume a value between 0 and 1, describes reaction of the volume of material to the presence of gases. When $\gamma = 0$, the presence of gases has no effect on the volume. When $\gamma = 1$, gases contribute to the volume of material in accordance with their densities. γ is calculated by volume-weighted averaging of the swelling factor specified for solids (γ_s) and liquids (γ_l):

$$\gamma = \frac{\gamma_s \sum_{s=1}^{N_s} \frac{m_s}{\rho_s} + \gamma_l \sum_{l=1}^{N_l} \frac{m_l}{\rho_l} + \tau \sum_{g=1}^{N_g} \frac{m_g}{\rho_g}}{\sum_{s=1}^{N_s} \frac{m_s}{\rho_s} + \sum_{l=1}^{N_l} \frac{m_l}{\rho_l} + \tau \sum_{g=1}^{N_g} \frac{m_g}{\rho_g}} \tag{4}$$

τ is a parameter that is used to ensure that, at the limit of very high gas content, the volume of material is defined by the densities of the gases.

Components may undergo reactions. Each reaction may have one or two reactants and zero to two products.

$$\theta_1 \, COMP1 \; + \; \theta_2 \, COMP2 \; \rightarrow \; \theta_3 \, COMP3 \; + \; \theta_4 \, COMP4 \; + \; h \tag{5}$$

The rate of reaction (r) taking place in a unit volume of material is defined by

$$r = A \exp\left(-\frac{E}{RT} \right) \left[\frac{m_{COMP1}}{V} \right] \left[\frac{m_{COMP2}}{V} \right] \tag{6}$$

where A and E are the Arrhenius pre-exponential factor and activation energy, and R is the gas constant. In the absence of the second reactant, $m_{COMP2} = V$. The rate of consumption or formation of a reactant or product is calculated by multiplying r by the corresponding stoichiometric coefficient (θ). The rate of production of heat is calculated by multiplying r by the heat of reaction (h). h is defined by the same type of temperature dependence as that used for

component properties (see equation 1). The reaction description also includes specification of a lower or upper temperature limit. If temperature decreases below the lower limit or increases above the upper limit, the rate of reaction is set to 0. Application of this limit increases computational efficiency (reaction rates are evaluated only at the temperatures where they are important) and facilitates usage of reactions for the description of phase transitions.

HEAT AND MASS TRANSFER.

The conduction of heat is described by Fourier's law

$$q = -kS\frac{\partial T}{\partial x}$$ (7)

where q is the rate of heat transfer, S is the surface area across that the heat is transferred, x is the coordinate normal to this surface. k is the thermal conductivity of material that depends on relative amounts and spatial distribution of components. If components are stacked in uniform layers that are normal to the direction of the heat flow, the thermal conductivity is

$$k_n = \frac{V}{\sum_{i=1}^{N_c}\frac{V_i}{k_i}}$$ (8)

where k_i and V_i are thermal conductivity and volume contribution of the i-th component. If the layers are parallel to the direction of the heat flow, the thermal conductivity is

$$k_p = \frac{\sum_{i=1}^{N_c}k_iV_i}{V}$$ (9)

The k_n and k_p expressions can be derived using an analogy with electric circuits consisting of resistors connected in series and parallel [9].

For an arbitrary spatial distribution of components, the exact analytical expression of the thermal conductivity is not available. However, under the assumption that components do not affect thermal conductivities of each other, equations 8 and 9 provide lower and upper limits for the value of k. This means that the thermal conductivity of material can be represented as

$$k = \beta k_p + (1-\beta)k_n$$ (10)

where β is a parameter that may assume a value between 0 and 1. In ThermaKin, this representation is used in conjunction with the assumption that a pyrolyzing material can be characterized by a single value of β.

3

The transfer of mass is assumed to be driven by a concentration gradient:

$$j_g = -\rho_g \lambda S \frac{\partial \left(\dfrac{(m_g / \rho_g)}{V} \right)}{\partial x} \tag{11}$$

where j_g is the rate of transfer of gas g (only gaseous components are considered to be mobile). λ is the gas transfer coefficient of material. It is calculated from the corresponding component coefficients using the same approach as that used for thermal conductivity (see equations 8-10). Note that λ does not depend on the nature of the gas that is being transferred (i.e., on volumetric basis, all gases subjected to the same concentration gradient are transferred with the same rate).

Application of Boyle's law, which states that the product of the pressure and volume of a fixed amount of gas is constant, transforms equation 11 into

$$j_g = -\frac{\rho_g \lambda S}{P^{def}} \frac{\partial (\phi P_g)}{\partial x} \tag{12}$$

where ϕ is the volume fraction of material occupied by gases, P_g is the partial pressure of gas g, and P^{def} is the pressure at which the gas density (ρ_g) is defined. If material is rigid and does not expand with addition of gases (i.e., $\gamma = 0$ and ϕ is constant), equation 12 assumes the form of Darcy's law, which is used to describe the flow of fluids through porous media [10]. However, if material expands proportionally to the volume of added gases (i.e., $\gamma > 0$ and pressure inside the material is constant), equation 12 states that the flow of gas is driven by the gradient of its volumetric fraction.

CONSERVATION EQUATIONS.

The overall behavior of a pyrolyzing object is described by mass and energy conservation equations. In ThermaKin, these equations are formulated in terms of rectangular finite elements. Each element is characterized by component masses and temperature. The formulation (described below) contains the following assumptions. The heat exchange between transferred gases and the rest of the material is instantaneous. The energy associated with the bulk velocity of gases and the work of expansion/contraction of material are negligible.

Consider an object consisting of two elements, L and R, shown in figure 1. An application of the law of conservation of mass to the g-th component in element R yields

$$\frac{\Delta m_g^R}{\Delta t} = V^R \sum_{j=1}^{N_r} \theta_j^g r_j^R + \lambda^{LR} \rho_g^{LR} S \frac{\left(\dfrac{(m_g^L / \rho_g^L)}{V^L} - \dfrac{(m_g^R / \rho_g^R)}{V^R} \right)}{\Delta x} \tag{13}$$

where $\Delta m_g{}^R$ is the change in the component mass during the time Δt. The terms on the right-hand side of the equation are contributions from reactions and mass transfer from element L (the mass transfer term is present only if component g is a gas). θ_j^g is the stoichiometric coefficient in front of component g in the j-th reaction. This coefficient is set to be negative when the component is a reactant and positive when it is a product. LR superscript is used to refer to averages of the parameters obtained for each of the two elements. Δx is the distance between the centers of the elements (see figure 1).
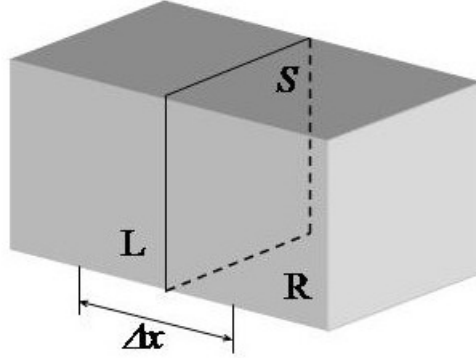

Figure 1. Two-Element Object

An application of the law of conservation of energy to element R yields

$$c^R \frac{\Delta T^R}{\Delta t} = V^R \sum_{j=1}^{N_r} h_j^R r_j^R + k^{LR} S \frac{\left(T^L - T^R\right)}{\Delta x} + \frac{1}{2} \sum_{g=1}^{N_g} c_g^{LR} \left(T^L - T^R\right) j_g^{LR} \qquad (14)$$

where ΔT^R is the change in the element temperature during the time Δt. The terms on the right-hand side of the equation account for heat generation by reactions, and conduction and convection of heat from element L. j_g^{LR} is the rate of flow of gas g from L to R (a detailed expression of this rate is given by the last term in equation 13).

The description provided by equations 13 and 14 is expanded to more complex systems in a straightforward manner. Addition of an element adjacent to element R results in addition of the terms that correspond to the flows of matter and energy from this element to the equations. To make this description complete, the conservation equations should be written for every component and every element of a pyrolyzing object and complemented by the conditions at the boundaries. The accuracy of the description strongly depends on the choice of element size and time step (Δt). This dependence is analyzed in section 4.

BOUNDARY CONDITIONS.

The one-dimensional version of ThermaKin has two boundaries, which can be viewed as top and bottom surfaces of a flat material object. Conditions at the boundaries are comprised of a description of mass and heat transfer through the boundary surfaces. Each boundary is described

separately using the following mathematical framework. The mass flow ($j_i{}^B$) of component i from the boundary element B is expressed as

$$j_i^B = \begin{cases} a_i \rho_i^B S^B \left(\dfrac{(m_i^B / \rho_i^B)}{V^B} - b_i \right) \\ \quad\quad\quad \text{or} \\ a_i S^B \exp\left(-\dfrac{b_i}{RT^B} \right) \end{cases}$$

(15)

where S^B is the surface area of the boundary, a_i and b_i are user-specified parameters, and R is the gas constant. The primary function of the linear expression is to remove or introduce gases from or to a pyrolyzing material. The exponential expression can be employed to simulate a surface reaction (such as oxidation) or dripping.

Convective heat flow ($q_c{}^B$) into the boundary element is defined by

$$q_c^B = v S^B \left(T^e - T^B \right)$$

$$T^e = T_0^e + T_t^e t$$

(16)

where v is the convection coefficient and T^e is the temperature outside of the material. This temperature can be a constant or a linear function of time (t). Radiative heat flow ($q_r{}^A$) into material is expressed as

$$q_r^A = \varepsilon^A S^B \left(f - \sigma \left(T^A \right)^4 \right)$$

$$f = \begin{cases} f_{10} + f_{1t} t & t \le t_1 \\ f_{20} + f_{2t} t & t_1 < t \le t_2 \end{cases}$$

(17)

where ε^A is emissivity of the element that absorbs radiation (element A), σ is the Stefan-Boltzmann constant, and f designates the flux of external radiation. It is defined by a sequence of two linear time dependencies, which can be specified to be periodic (i.e., the flux history can be repeated with the period of t_2).

The element that absorbs radiation is determined at every time step using either a maximum absorption or a random absorption algorithm. In both cases, the external radiation is assumed to penetrate material in the direction normal to the boundary surface and behave in accordance with Beer-Lambert's law [11]:

$$f^A = f^I a^A l^A$$

(18)

Where f^{I} is the flux entering the element A, f^{A} is the flux absorbed by the element, a^{A} is absorbance, and l^{A} is thickness of the element. When the maximum absorption algorithm is employed, the element that, according to equation 18, absorbs most of the radiation is assumed to absorb all of it. In the case of the random absorption algorithm, the absorbing element is selected at random using the Beer-Lambert distribution of absorbed energy as a probability density guiding this selection. In both approaches, the absorbing element also acts as a gray body reflector and emitter (see equation 17). The emissivity and absorbance used in equations 17 and 18 are calculated from component emissivities (ε_i) and absorption coefficients (α_i):

$$\varepsilon = \frac{\sum_{i=1}^{N_c} \varepsilon_i V_i}{V} \tag{19}$$

$$a = \frac{\sum_{i=1}^{N_c} \alpha_i m_i}{V} \tag{20}$$

The ThermaKin boundary conditions are also equipped with a submodel simulating surface ignition. The criterion for the ignition (CI) is based on component mass fluxes:

$$\mathrm{CI} = \sum_{i=1}^{N_c} \frac{(j_i^{\mathrm{B}} / S^{\mathrm{B}})}{\xi_i} \tag{21}$$

where ξ_i is a user-specified critical mass flux of component i. When CI is above 1, the flame is turned on. The radiative heat flux from the flame, defined by a constant, is added to the external heat flux f. At the same time, convective heat transfer parameters v and T^{e} are replaced by constant parameters describing the flaming conditions.

SOLUTION METHODOLOGY.

The equations formulated in the Conservation Equations section can be cast into the following general form:

$$y_i^{t+\Delta t} = y_i^t + F_i(y_i, y_j, y_k, ...)\Delta t \tag{22}$$

where $y_i^{t+\Delta t}$ is component mass or temperature in some element E at the time $t+\Delta t$. $y_i^{t+\Delta t}$ is unknown and needs to be determined from the value of this parameter (y_i^t) at the current time (t) and the rate, F_i, with which this parameter changes. F_i is a function of component masses and temperatures ($y_i, y_j, y_k, ...$) in element E and adjacent elements. F_i also implicitly depends on time and can be approximated by the average of its values at t and $t+\Delta t$:

$$y_i^{t+\Delta t} = y_i^t + \frac{\left[F_i(y_i^t, y_j^t, y_k^t, ...) + F_i(y_i^{t+\Delta t}, y_j^{t+\Delta t}, y_k^{t+\Delta t}, ...)\right]}{2}\Delta t \tag{23}$$

7

This approach is called the Crank-Nicolson scheme [12].

Equation 23, written for every component mass and temperature of every element, forms a set of coupled algebraic equations. These equations are nonlinear in nature and, therefore, are difficult to solve. To rectify this problem, function F_i at $t+\Delta t$ is linearized by using the first two terms of the Taylor series:

$$F_i^{t+\Delta t} = F_i^t + \frac{\partial F_i^t}{\partial y_i}(y_i^{t+\Delta t} - y_i^t) + \frac{\partial F_i^t}{\partial y_j}(y_j^{t+\Delta t} - y_j^t) + \frac{\partial F_i^t}{\partial y_k}(y_k^{t+\Delta t} - y_k^t) + \dots \qquad (24)$$

Substitution of the linearized function into equation 23 produces a system of linear equations that has block tridiagonal character. These equations are solved (to obtain $y_i^{t+\Delta t}$, $y_j^{t+\Delta t}$, $y_k^{t+\Delta t}$,...) using an approach similar to LU decomposition with iterative improvement of the solution [13]. Solving these equations constitutes performance of an integration time step.

Note that, as a result of the integration, the sizes of elements may change. These changes, accumulated over time, may have substantial negative effects on the accuracy of the solution procedure. To minimize these effects, element sizes are adjusted after every time step. If an element is larger than a preset size, it is split in two. If it is smaller, a fraction of the following element is added to bring it to the preset size. The temperature of the mixed element is recalculated to ensure the conservation of energy.

The solution procedure described above is used in the one-dimensional version of ThermaKin (it is expected to be modified somewhat for multidimensional cases). This procedure has been implemented as a C++ program. An overview of the structure of the program can be found in appendix A. A detailed description of the program input and output is given in appendix B.

MODEL VERIFICATION

The ability of ThermaKin to predict experimental observations will be tested in future studies. In this work, the key submodels of ThermaKin have been verified by comparing the results of numerical calculations with analytical solutions. The heat transfer submodel has been tested against analytical solutions for conduction in a semi-infinite solid and in-depth absorption of radiation. The reactions submodel has been checked against an analytical solution for four coupled first and second order reactions. The mass transfer submodel has been verified against an analytical solution for diffusion from a thin layer.

8

CONDUCTION IN SEMI-INFINITE SOLID.

The temperature (T) of a semi-infinite solid that is heated at the boundary surface by convection can be expressed [14] as

$$\frac{T - T^i}{T^e - T^i} = 1 - \mathrm{erf}\left(\frac{x}{2\sqrt{X}}\right) - \exp\left(\frac{vx}{k} + \frac{v^2 X}{k^2}\right)\left(1 - \mathrm{erf}\left(\frac{x}{2\sqrt{X}} + \frac{v\sqrt{X}}{k}\right)\right)$$

$$X = \frac{k}{\rho c} t$$

(25)

where T^i is the initial temperature of the solid, and T^e is the temperature outside of the solid. For $\rho = 1000$ kg m^{-3}, $c = 2000$ J kg^{-1} K^{-1}, $k = 0.2$ W m^{-1} K^{-1}, $v = 90$ W m^{-2} K^{-1}, $T^i = 300$ K, and $T^e = 900$ K, this expression is plotted in figure 2 together with the results of ThermaKin calculations (performed using identical set of properties and conditions). A 0.04-m thick slab of material with no heat exchange at one of the boundaries was used in ThermaKin to simulate the infinite solid. The element size and time step were set at 2×10^{-5} m and 0.05 s, respectively. A factor of five increase in either integration parameter produced no noticeable changes in the results. With the exception of a small discrepancy between $t = 450$ s curves, the analytical and ThermaKin temperatures are indistinguishable. The discrepancy is a consequence of a limited accuracy of the spreadsheet program that was used to calculate the analytical temperatures.
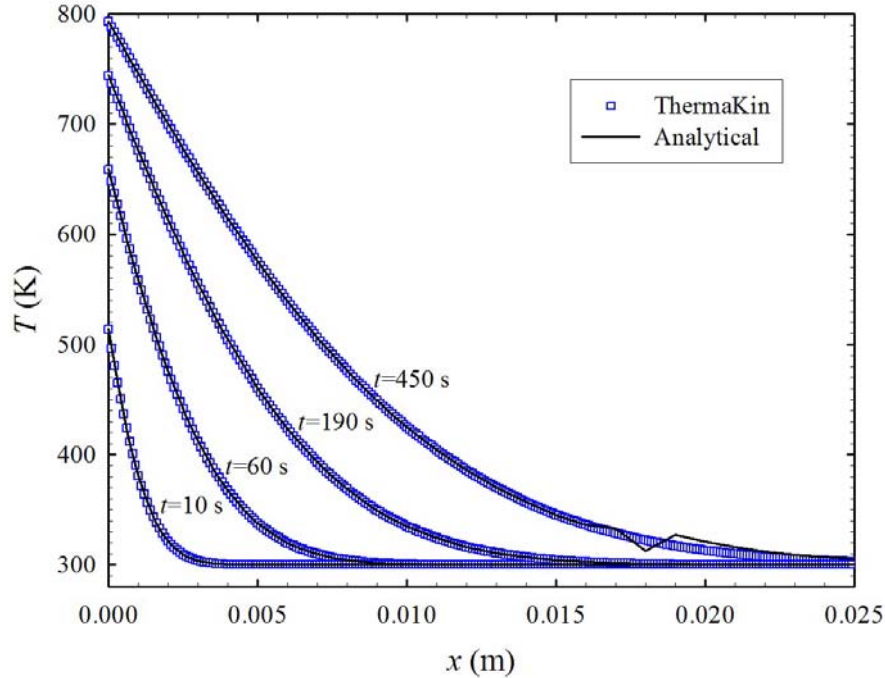

Figure 2. Comparison of Analytical and ThermaKin Solutions for Conduction in Semi-Infinite Solid

IN-DEPTH ABSORPTION OF RADIATION.

According to Beer-Lambert law [11], the density of energy (Φ) delivered into a material by radiation during a period of time t can be calculated as

$$\Phi = f^i \alpha \rho \exp(-\alpha \rho x) t \tag{26}$$

where f^i is the radiative heat flux that penetrates the surface of the material. To determine whether the random absorption algorithm (described in the Boundary Conditions section) provides an adequate description of the radiative energy transfer, ThermaKin calculations were performed on a 0.003-m thick layer of material exposed to 5×10^4 W m^{-2} radiative heat flux. The boundary conditions were formulated in such a way that all radiation was absorbed and none of it was reemitted. The material was characterized by $\rho = 1000$ kg m^{-3}, $c = 2000$ J kg^{-1} K^{-1}, and $\alpha = 3$ m^2 kg^{-1}. The thermal conductivity was set to a negligibly small value (1×10^{-10} W m^{-1} K^{-1}) to prevent nonradiative energy transfer. The simulations were run for 10 s using 0.05- and 0.001-s time steps. The element size was set at 2×10^{-5} m.

The energy densities obtained from the ThermaKin simulations are compared with those calculated using equation 26 in figure 3. The ThermaKin energy densities were obtained by multiplying increases in local temperatures (achieved as a result of 10 s exposure) by the product of ρ and c. The large time step simulation produces a noisy energy pattern because of a small number of times (200) the Beer-Lambert distribution is sampled. When the number is increased to 10000 (the small time step simulation), ThermaKin energy distribution becomes closely aligned with the analytical result.
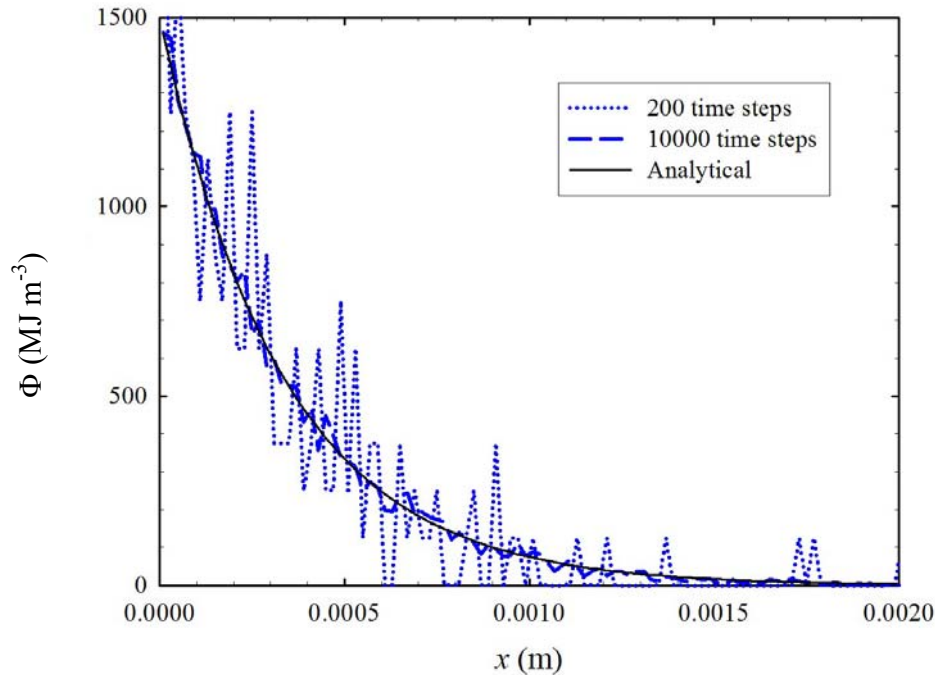

Figure 3. Comparison of Analytical and ThermaKin Distributions of Absorbed Radiative Energy

CHEMICAL REACTIONS.

Consider the following set of chemical reactions

$$1\,C \;\rightarrow\; 1\,PC \tag{27}$$

$$0.5\,C \;+\; 0.5\,C \;\rightarrow\; 1\,PCC \tag{28}$$

$$1\,D \;\rightarrow\; 1\,PD \tag{29}$$

$$1\,D \;+\; 0\,C \;\rightarrow\; 1\,PD \tag{30}$$

where C and D are reactants, and PC, PCC, and PD are products. The reactions are assumed to obey the rate law described in the Components and Reactions section. The temperature of the system is set to be constant. Note that, while C is not consumed in reaction 30, the rate of this reaction depends on the amount of C (in accordance with equation 6). Under these conditions, a straightforward integration of the rate equations becomes possible:

$$[C]_t = \frac{[C]_0 \, rk_{27} \exp(-rk_{27}t)}{[C]_0 \, rk_{28}(1 - \exp(-rk_{27}t)) + rk_{27}} \tag{31}$$

$$[PC]_t = [PC]_0 + \frac{rk_{27}}{rk_{28}} \ln\left([C]_0 \frac{rk_{28}}{rk_{27}} (1 - \exp(-rk_{27}t)) + 1 \right) \tag{32}$$

$$[PCC]_t = [PCC]_0 + [C]_0 - [C]_t - [PC]_t + [PC]_0 \tag{33}$$

$$[D]_t = [D]_0 \exp(-rk_{29}t)\left(\frac{rk_{27}}{[C]_0 \, rk_{28}(1 - \exp(-rk_{27}t)) + rk_{27}} \right)^{\frac{rk_{30}}{rk_{28}}} \tag{34}$$

$$[PD]_t = [PD]_0 + [D]_0 - [D]_t \tag{35}$$

Square brackets are used to indicate initial (subscript 0) or current (subscript t) concentrations of components. rk_{27}, rk_{28}, rk_{29}, and rk_{30} are rate constants of the corresponding reactions. Each rate constant represents the product of the pre-exponential factor and exponent in equation 6.

For $[C]_0$ = 990 kg m^{-3}, $[D]_0$ = 10 kg m^{-3}, $[PC]_0$ = $[PCC]_0$ = $[PD]_0$ = 0, rk_{27} = 0.02 s^{-1}, rk_{28} = 1×10^{-4} m^3 kg^{-1} s^{-1}, rk_{29} = 0.002 s^{-1}, and rk_{30} = 5×10^{-5} m^3 kg^{-1} s^{-1}, analytically calculated concentration histories are plotted in figure 4. The ThermaKin solution obtained for identical conditions using a single isolated element to represent the chemical system is also shown in the figure. The results of the ThermaKin calculations (performed using 0.05-s time step) are in excellent agreement with the analytical solution.
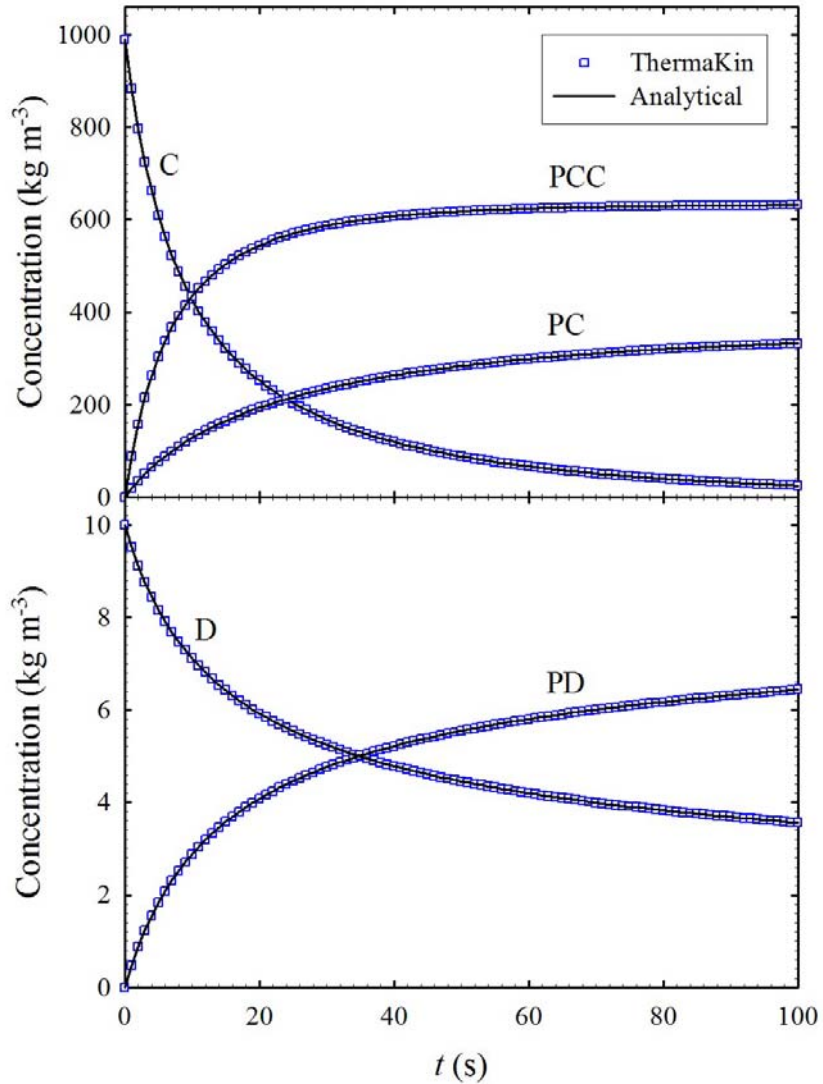
Figure 4. Comparison of Analytical and ThermaKin Solutions for a System of Chemical Reactions

DIFFUSION FROM A THIN LAYER.

When component C is introduced into a very thin layer of material that consists of component D, the subsequent one-dimensional diffusion of C can be described [15] by

$$[C] = \frac{M_C}{2\sqrt{\pi d_{CD} t}} \exp\left(-\frac{(x - x_C^i)^2}{4 d_{CD} t}\right) \tag{36}$$

where [C] is the concentration of C, M_C is the total amount of C per unit area, d_{CD} is the diffusion coefficient of C in D, and x_C^i is the position of the thin layer. A ThermaKin model of this process was comprised of 0.03-m thick slab of solid component D held at a constant temperature

with no mass transfer at the boundaries. Two hundred and twenty grams per square meter (0.22 kg m^{-2}) of gaseous component C was placed into a single element located in the center of the slab. The swelling factor for solid components (γ_s) was set to 0. This means that only component D (the density of which was set at 1000 kg m^{-3}) contributed to the material's volume. The gas transfer coefficient for D (λ_D), which is, under these conditions, equivalent to the diffusion coefficient d_{CD}, was set at 8×10^{-8} m^2 s^{-1}.

A comparison of the results of the ThermaKin calculations with those obtained using equation 36 is shown in figure 5. The ThermaKin results, which were computed using 2×10^{-5} m element size and 0.001-s time step, are in excellent agreement with the analytical solution. A factor of five increase in either of the integration parameters produced no noticeable changes in the results.
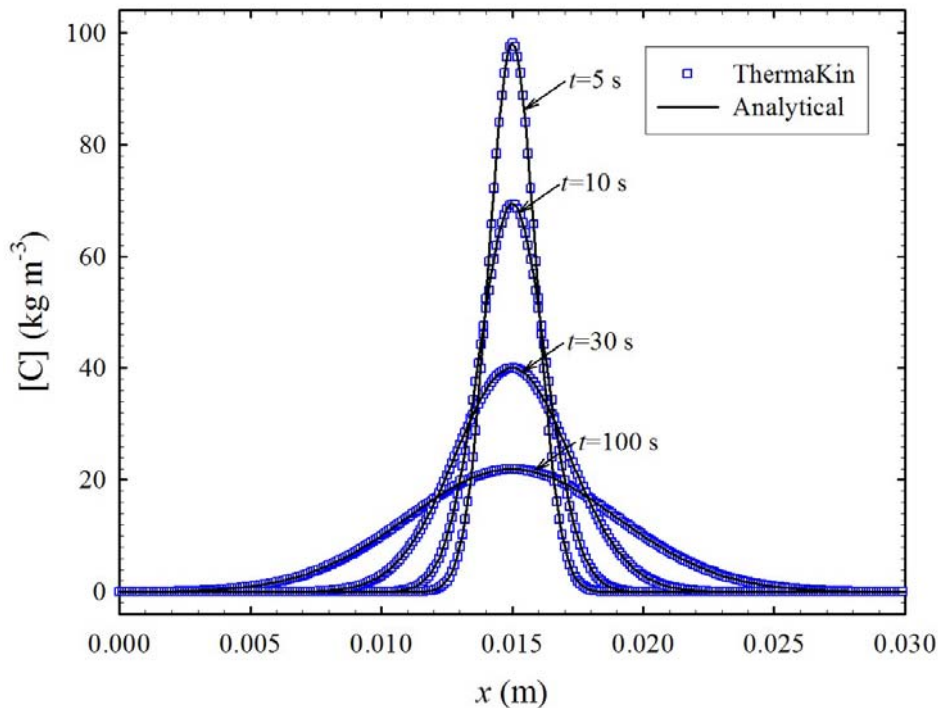

Figure 5. Comparison of Analytical and ThermaKin Solutions for Diffusion From a Thin Layer

COMPUTATIONAL COSTS

The computational cost of a ThermaKin calculation depends on the size of a material object, length of simulation, and choice of integration parameters. The parameter values are dictated by the scales of the processes that need to be resolved. The goal of the analysis described below was to determine element size, time step, and the amount of computer resources that provide the converged solution for what could be considered as a typical one-dimensional pyrolysis problem. All calculations (including those described in the previous section) were performed on a PC equipped with a 3.4 gigahertz Intel® Xeon® (single core) processor, 2 gigabyte of random-access memory, and Microsoft® Windows XP® operating system. The ThermaKin program was compiled using Microsoft Visual C++ .NET® nonoptimizing compiler.

13

The material used in these calculations was defined by the following properties: $\rho = 1000$ kg m^{-3}, $c = 500+3T$ J kg^{-1} K^{-1}, $k = 0.2$ W m^{-1} K^{-1}, and $\varepsilon = 0.95$. Decomposition of this material was assumed to occur in a single step first order endothermic reaction. The Arrhenius pre-exponential factor, activation energy, and heat of reaction were set at 5×10^{15} s^{-1}, 2.5×10^5 J mol^{-1}, and -1×10^6 J kg^{-1}, respectively. The stoichiometric coefficient of the reactant (the material) was equal to 1. No product was specified. The products of the decomposition were assumed to leave the material instantaneously.

One side of 0.005-m thick layer of this material, which was initially at 300 K, was irradiated by 5×10^4 W m^{-2} heat flux. Application of the maximum absorption algorithm and a high absorption coefficient (1000 m^2 kg^{-1}) ensured that the radiation was absorbed at the surface. The convective heat transfer at the surface was defined by $T^e = 300$ K and $v = 10$ W m^{-2} K^{-1} (see equation 16). The other side of the material layer was thermally insulated. This was achieved by turning off external heat fluxes and adding a boundary element consisting of a nondegradable material with $k = 1 \times 10^{-10}$ W m^{-1} K^{-1} and $\varepsilon = 0$. All mass transfer was turned off.

For 1×10^{-5} m element size and 0.01-s time step, the rate of mass loss, which is probably the most important descriptor of a pyrolysis process, is shown in figure 6. An order of magnitude increase in element size produces no significant changes in the rate history, which means that for this range of element sizes the solution is converged. Further increase in element size to 5×10^{-4} m yields a diverged solution (see figure 6). The results of a similar analysis applied to time step are depicted in figure 7. With element size fixed at 1×10^{-5} m, the integration diverges when time step is increased to 2 s. When element size is set at a higher value of 1×10^{-4} m, the divergence does not occur until time step reaches 20 s. On the basis of these analyses, it can be concluded that a combination of 3×10^{-5} m element size and 0.1-s time step should be more than sufficient to produce a converged solution for this type of pyrolysis problem. A 400-s simulation performed using these integration parameters required about 30 s of the computer time.
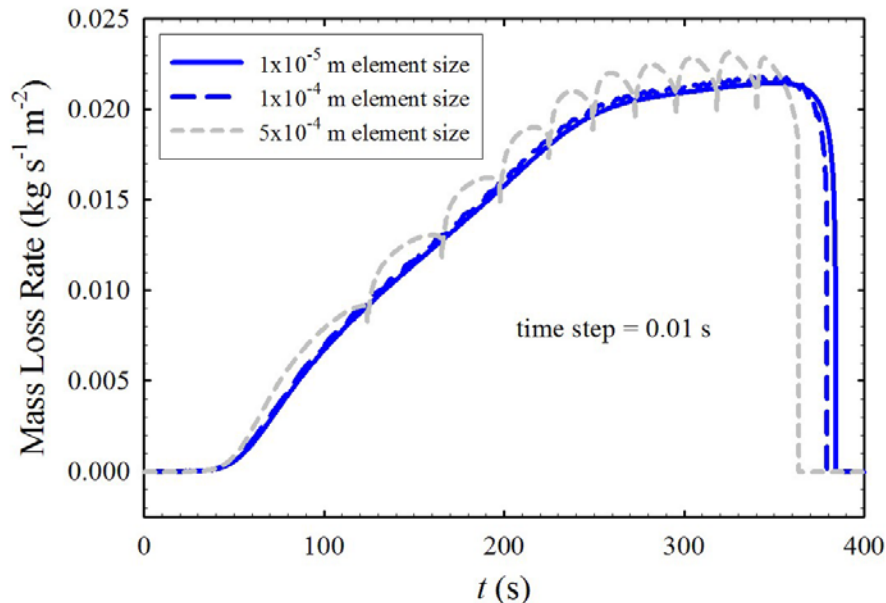

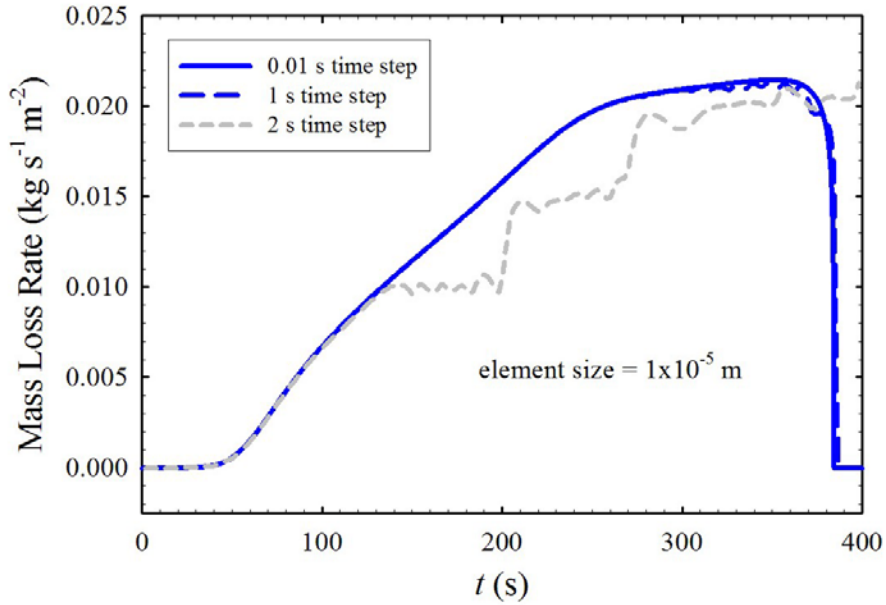Figure 6. Dependence of Mass Loss Rate History on Element Size

14

Figure 7. Dependence of Mass Loss Rate History on Time Step

Two potentially important aspects of materials behavior that were omitted from the previous results are in-depth absorption of radiation and charring. To understand whether these phenomena have a significant effect on the convergence of the solution, several additional calculations were performed. First, the absorption coefficient of the material was reduced to 3 m^2 kg^{-1}, and the random absorption algorithm (simulating Beer-Lambert distribution of absorbed energy) was turned on. This means that the material became partially transparent to external radiation (approximately 95% of the radiation was absorbed by the first 0.001 m of the material layer). The rest of the properties and conditions were kept the same as specified previously. The results of these calculations performed using 3×10^{-5} m element size and 0.1-time step are shown in figure 8. The mass loss rate is rather noisy indicating that the time step may not provide a sufficiently high rate of sampling for the random absorption algorithm. An order of magnitude decrease in the time step brings the noise to an acceptable level and increases the computer time to 240 s. Note that this relatively small adjustment in the manner in which external radiation is absorbed results in a significant change in the mass loss rate history (see figure 8).
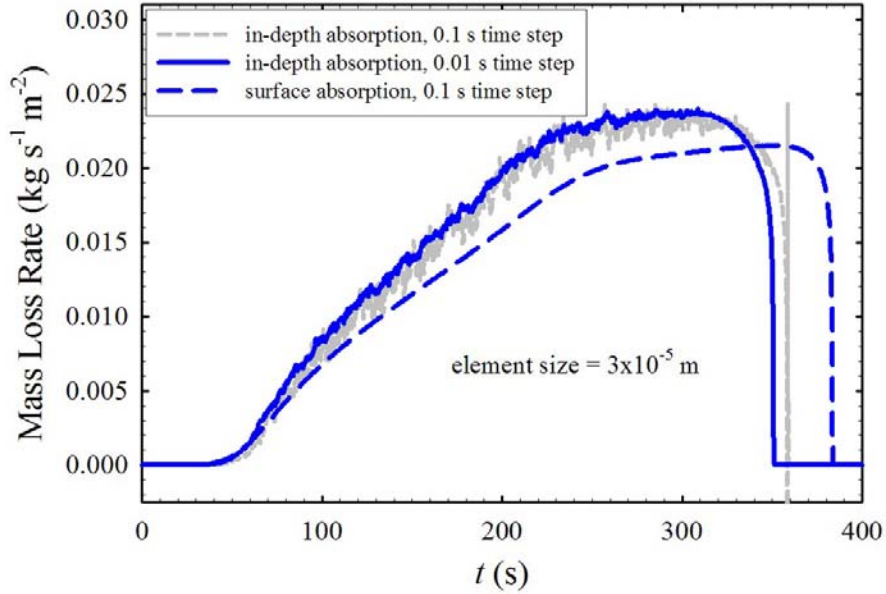
Figure 8. Effects of In-Depth Absorption and Time Step on Mass Loss Rate History

In the second set of calculations, in-depth absorption of radiation was turned off. Instead, the pyrolysis model was augmented to include production of intumescent char. This was done by specifying a product for the material decomposition reaction. The product was assigned a stoichiometric coefficient of 0.25 (25% by mass char yield). With the exception of the density that was set at 50 kg m^{-3}, all physical properties of this product were defined to be the same as the original material. The low density of the product was used to simulate expansion of the material during pyrolysis. The stoichiometry and density were chosen so that the thickness of the material increased by a factor of five (to 0.025 m) as a result of the decomposition. The results of the calculations performed on this model using 3×10^{-5} m element size and 0.1 time step are shown in figure 9. A factor of five increase in either of the integration parameters produced no noticeable changes in the mass loss rate history. This indicates that the intumescence has no significant effect on the convergence of the solution. Note that it takes much longer (about 1700 s) for the material to pyrolyze because of an insulating effect of the char. The computer time also increases substantially, to 660 s, due to a combined effect of the increases in the length of simulation and thickness of material.
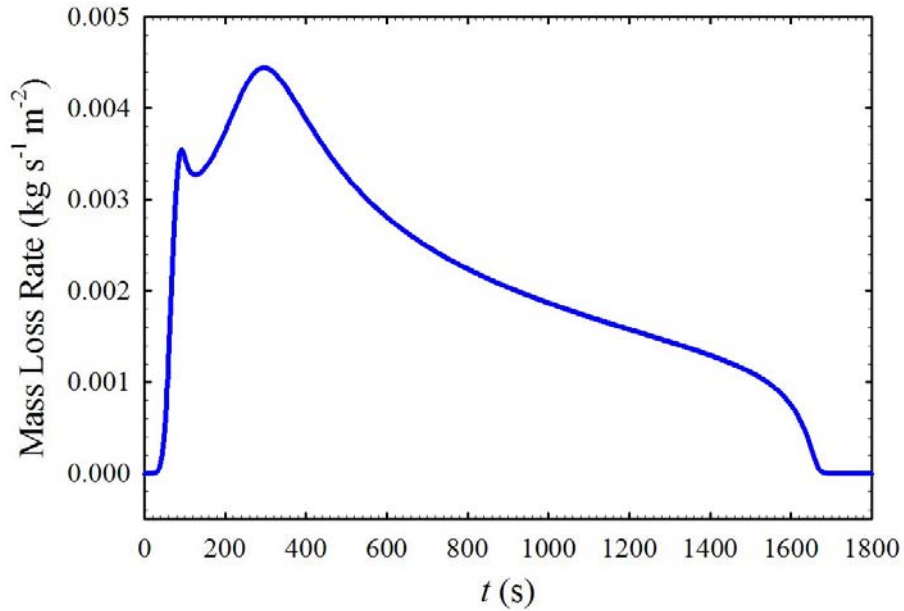
Figure 9. Mass Loss Rate History of a Charring Material

CONCLUSIONS

A versatile numerical model (called ThermaKin) of pyrolysis and combustion of polymeric materials has been formulated. The one-dimensional version of this model has been implemented as a C++ program and verified by comparing its results with analytical solutions. The computational costs of pyrolysis simulations performed using this program were found to be low. Future work will be focused on using ThermaKin to develop fundamental property-based descriptions that provide an accurate prediction of materials fire behavior.

REFERENCES

1. Staggs, J.E.J., "A Theory for Quasi-Steady Single-Step Thermal Degradation of Polymers," *Fire and Materials*, Vol. 22, 1998, pp. 109-118.

2. Lyon, R.E., "Heat Release Kinetics," *Fire and Materials*, Vol. 24, 2000, pp. 179-186.

3. Di Blasi, C., "Analysis of Convection and Secondary Reaction Effects Within Porous Solid Fuels Undergoing Pyrolysis," *Combustion Science and Technology*, Vol. 90, 1993, pp. 315-340.

4. Staggs, J.E.J., "A Simple Model of Polymer Pyrolysis Including Transport of Volatiles," *Fire Safety Journal*, Vol. 34, 2000, pp. 69-80.

5. Agrawal, S. and Atreya, A., "Wind-Aided Flame Spread Over an Unsteadily Vaporizing Solid," *Twenty-Fourth Symposium (International) on Combustion*, 1992, pp. 1685-1693.

6. Di Blasi, C., "Processes of Flames Spreading Over the Surface of Charring Fuels: Effects of the Solid Thickness," *Combustion and Flame*, Vol. 97, 1994, pp. 225-239.

7. ASTM Standard E 1354-04, "Standard Test Method for Heat and Visible Smoke Release Rates for Materials and Products Using an Oxygen Consumption Calorimeter," American Society for Testing and Materials, West Conshohocken, PA, 2004.

8. ASTM Standard E 906-06, "Standard Test Method for Heat and Visible Smoke Release Rates for Materials and Products Using a Thermopile Method," American Society for Testing and Materials, West Conshohocken, PA, 2006.

9. Holman, J.P., *Heat Transfer*, McGraw-Hill, Boston, MA, 2002, pp. 25-70.

10. Scheidegger, A.E., *The Physics of Flow Through Porous Media*, University of Toronto Press, Toronto, Canada, 1974, pp. 73-98.

11. Atkins, P.W., *Physical Chemistry*, W.H. Freeman and Company, San Francisco, CA, 1978, pp. 582-611.

12. Press, W.H., Teukolsky, S.A., Vetterling, W.T., and Flannery, B.P., *Numerical Recipes in C++: The Art of Scientific Computing*, Cambridge University Press, Cambridge, UK, 2002, pp. 829-890.

13. Press, W.H., Teukolsky, S.A., Vetterling, W.T., and Flannery, B.P., *Numerical Recipes in C++: The Art of Scientific Computing*, Cambridge University Press, Cambridge, UK, 2002, pp. 35-107.

14. Holman, J.P., *Heat Transfer*, McGraw-Hill, Boston, MA, 2002, pp. 131-204.

15. Middleman S., *An Introduction to Mass and Heat Transfer: Principles of Analysis and Design*, John Wiley & Sons, Inc., New York, NY, 1998, pp. 109-203.

APPENDIX A—PROGRAM STRUCTURE

The ThermaKin program was written using the ANSI/ISO C++ and its standard library. The program should compile on any platform for which the standard C++ is available. The key modules of this program, their functions, and interactions are shown in figure A-1. OneD is the module that contains an array of structures describing elements of a one-dimensional object. Every time step, mat, topB, and botB modules calculate the rates (and derivatives of the rates) of changes in component masses and temperatures of each element. Subsequently, OneD module compiles this information into a system of linear equations and sends it to LES module, which solves these equations. After new element masses and temperatures are determined, OneD module adjusts element sizes and, if requested, reports information on the new state of the material object to IO module. This routine is repeated until the specified simulation time is reached.
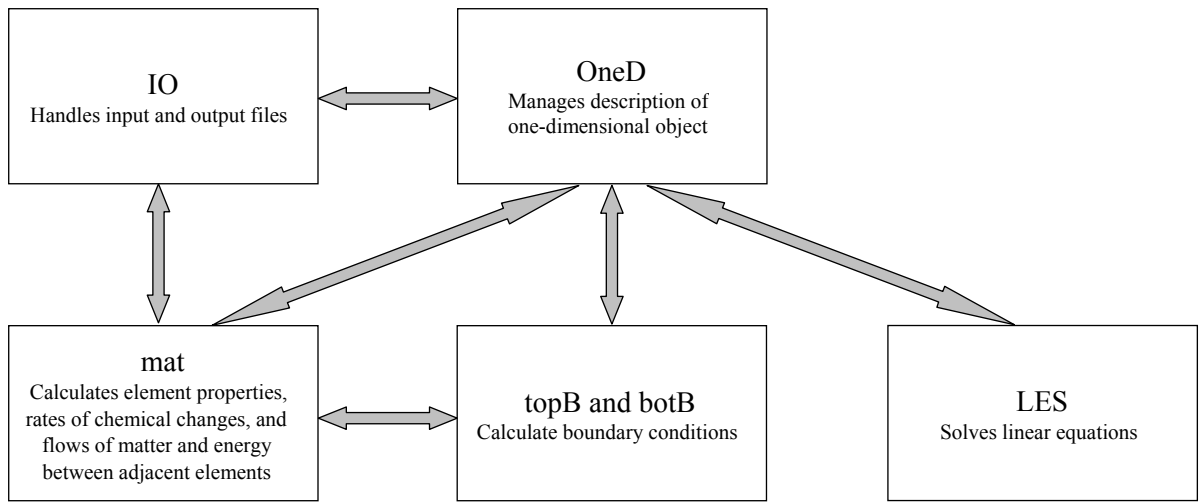
Figure A-1. Key Modules of ThermaKin Program

APPENDIX B—INPUT AND OUTPUT

When the ThermaKin program starts, it asks for three file names. The information on components and reactions is read from components file. The information on the initial state of a material object, boundary conditions, and integration parameters is read from conditions file. The last name is that of a new file where the calculation results are output. Both input and output files have a simple text format. The input is case sensitive. With a few exceptions indicated below, all numerical parameters in the input files are in the units based on kg, m, s, K, and J. The current version of ThermaKin, version 1, does not have any parameter checking algorithms. It is a responsibility of the user to make sure that, within the range of conditions encountered in a given simulation, the parameters are meaningful.

The specification of a component starts with its name (single word), followed by its state (S for solid, L for liquid, or G for gas), and properties:

```
COMPONENT:        COMP1
STATE:            S
DENSITY:          1000  0 0 0
HEAT CAPACITY:    500   3 0 0
CONDUCTIVITY:     0.2   0 0 0
TRANSPORT:        1e-10 0 0 0
EMISSIVITY & ABSORPTION: 0.95  1000
```

Density, heat capacity, thermal conductivity, and gas transfer coefficient (TRANSPORT) are defined by specifying parameters of equation 1 in the following order: p_0, p_1, p_n, and n. Emissivity and absorption coefficient are defined by single values. The current version of ThermaKin allows up to 20 components. Their specifications should be separated by at least one space.

Chemical interactions between components are defined as follows:

```
REACTION:         COMP1 + COMP2 -> COMP3 + NOCOMP
STOICHIOMETRY:    1        0.25       1.25      0
ARRHENIUS:        5e15  2.5e5
HEAT:             -1e6  0 0 0
TEMP LIMIT:       L     400
```

If the program encounters a component that is not specified (NOCOMP), it omits this component from the reaction definition. Stoichiometric coefficients θ (see equation 5) are specified in the same order as the corresponding component names in the reaction equation. The stoichiometry is followed by the Arrhenius parameters A and E (see equation 6). E has the units of J mol^{-1}. The heat of reaction (HEAT) is defined by parameters of equation 1 (p_0, p_1, p_n, and n). The last parameter in the reaction description is the upper (U) or lower (L) temperature limit (the limit above or below which the rate of reaction is set to 0). The current version of ThermaKin allows up to 20 reactions. Their specifications should be separated by at least one space.

The components file may also contain a description of physical interactions between components:

MIXTURES
S SWELLING: 0
L SWELLING:
G SWELLING LIMIT: 1e-10
PARALL CONDUCTIVITY: 0.5
PARALL TRANSPORT: 0.5

This description includes the values of γ_s (S SWELLING), γ_l (L SWELLING), and τ (G SWELLING LIMIT) parameters, which are used in the calculation of material's swelling factor (see equation 4). The last 2 parameters in the description define the weight of parallel averaging (parameter β in equation 10) in the calculations of the thermal conductivity and gas transfer coefficient of material.

The conditions file begins with a definition of model geometry:

OBJECT TYPE: 1D

In the current version of ThermaKin, one-dimensional object is the only option. This is followed by specification of the initial state of the object:

OBJECT STRUCTURE

THICKNESS: 0.005
TEMPERATURE: 300
MASS FRACTIONS:
COMP1   0.9
COMP2   0.1

THICKNESS: 0.001
TEMPERATURE: 300
MASS FRACTIONS:
COMP1   0.1
COMP2   0.9

A one-dimensional object is assumed to consist of layers. Any number of layers can be specified. Each layer is characterized by thickness, temperature, and mass fractions of components.

After the object structure, boundary conditions are defined:

OBJECT BOUNDARIES

TOP BOUNDARY
MASS TRANSPORT: YES
COMP2   LIN   0.1   0.3
COMP3   EXP   1e17   3e5

OUTSIDE TEMP TIME PROG: 300   0
CONVECTION COEFF: 15

EXTERNAL RADIATION: YES
TIME PROG1:   5e4   20   500
TIME PROG2:   6e4   -20   500
REPEAT: NO
ABSORPTION MODE: MAX

FLAME: YES
IGNITION MASS FLUXES:
COMP2   0.01
COMP3   0.02
OUTSIDE TEMP: 1400
CONVECTION COEFF: 20
RADIATION: 2.5e4

BOTTOM BOUNDARY

MASS TRANSPORT: NO

OUTSIDE TEMP TIME PROG: 300   0.1
CONVECTION COEFF: 5

EXTERNAL RADIATION: NO

FLAME: NO

The definition of the top boundary, which corresponds to the layer of material specified first in the object structure, is followed by that of the bottom boundary. These definitions have identical format. Component mass flows (MASS TRANSPORT) are defined by listing the name of component, type of expression (LIN for linear or EXP for exponential), and values of parameters *a* and *b* used in the expression (see equation 15). When exponential form of the mass flow expression is used, *b* has the units of J mol^{-1}. Turning off mass flow (MASS TRANSPORT: NO) at both boundaries also turns off mass transfer inside material.

The convective heat flow across a boundary is defined by specifying outside temperature T^e and convection coefficient v (see equation 16). The outside temperature is expressed as a linear function of time (OUTSIDE TEMP TIME PROG). This function is defined by the initial temperature value followed by the rate at which this temperature changes. The flux of external radiation f (see equation 17) is defined by a sequence 2 linear time dependencies (TIME PROG1 and TIME PROG2). Each of these dependencies is defined by the initial flux value, the rate of change of the flux and the length of time during which the dependence is followed. If the sequence is specified to repeat itself (REPEAT: YES), the program will do it for as long as the simulation is run. On the other hand, if the repeat is turned off (REPEAT: NO) and the sequence is complete, the external heat flux resets to 0. The last parameter in the external radiation specification (ABSORPTION MODE) is used to select between the maximum (MAX) and random (RAND) radiation absorption algorithms (they are described in the Boundary Conditions section). When external radiation is turned off (EXTERNAL RADIATION: NO), the maximum radiation absorption algorithm is used by default.

The last set of entries defining a boundary (beginning with FLAME keyword) describe surface ignition. First, critical (IGNITION) mass fluxes ξ (see equation 21) are listed next to the corresponding component names. Those components that are not listed are assumed to have infinite ξ. Next, convective heat transfer parameters T^e and v describing the flaming conditions are specified (T^e in this case is a constant). The last parameter (RADIATION) is the radiative heat flux from the flame. This flux is added to the external heat flux f, when the flame is on.

The top and bottom boundaries are mathematically identical in all aspects, except one. When element sizes are adjusted (using an algorithm described in the Solution Methodology section), the adjustment procedure always starts from the bottom boundary element and proceeds to the top. To minimize object structure distortions caused by this procedure, the object side experiencing the most significant shrinkage or expansion should be bound by the top boundary.

The conditions file is completed by specifying integration and output parameters:

INTEGRATION PARAMETERS

ELEMENT SIZE: 3e-5
TIME STEP: 0.1
DURATION: 1

OUTPUT FREQUENCY:
ELEMENTS: 10
TIME STEPS: 10

Element size, time step, and the length (DURATION) of simulation are followed by output frequencies. In the example shown above, information on the state of the object will be output every 10 time steps. The output will include specification of location, temperature, and composition of every tenth element of the object. An example of ThermaKin output file is given below. All information contained in this file is clearly defined and does not require any further explanation.

ThermaKin Program Version 1

Components file: pyrochar.cmp
Conditions file: pyrochar.cnd
Number of components: 2
Number of reactions: 1
Mixture rules assigned: yes

Object type: 1D
Number of layers: 1

Top Boundary
External radiation: on
Mass transport: off
Ignition: off

Bottom Boundary
External radiation: off
Mass transport: off
Ignition: off

****

Time [s] = 0.000000e+000

BOUNDARY	AREA [m^2]	HEAT FLOW IN [J/s]	MASS FLOW OUT [kg/s]:	
			POLYM	CHAR
TOP	1.000000e+000	4.213320e+004	0.000000e+000	0.000000e+000
BOTTOM	1.000000e+000	-3.366800e+003	0.000000e+000	0.000000e+000

FROM TOP [m]	TEMPERATURE [K]	CONCENTRATION [kg/m^3]:	
		POLYM	CHAR
1.000000e-005	5.000000e+002	1.000000e+003	0.000000e+000
3.050000e-004	5.000000e+002	1.000000e+003	0.000000e+000
6.050000e-004	5.000000e+002	1.000000e+003	0.000000e+000
9.050000e-004	5.000000e+002	1.000000e+003	0.000000e+000
1.205000e-003	5.000000e+002	1.000000e+003	0.000000e+000
1.505000e-003	5.000000e+002	1.000000e+003	0.000000e+000
1.805000e-003	5.000000e+002	1.000000e+003	0.000000e+000
2.105000e-003	5.000000e+002	1.000000e+003	0.000000e+000
2.405000e-003	5.000000e+002	1.000000e+003	0.000000e+000
2.705000e-003	5.000000e+002	1.000000e+003	0.000000e+000
3.005000e-003	5.000000e+002	1.000000e+003	0.000000e+000
3.305000e-003	5.000000e+002	1.000000e+003	0.000000e+000
3.605000e-003	5.000000e+002	1.000000e+003	0.000000e+000
3.905000e-003	5.000000e+002	1.000000e+003	0.000000e+000

4.205000e-003	5.000000e+002	1.000000e+003	0.000000e+000
4.505000e-003	5.000000e+002	1.000000e+003	0.000000e+000
4.805000e-003	5.000000e+002	1.000000e+003	0.000000e+000
4.985000e-003	5.000000e+002	1.000000e+003	0.000000e+000

Total thickness [m] = 5.000000e-003
Total mass [kg/m^2] = 5.000000e+000

****

Time [s] = 1.000000e+000

BOUNDARY	AREA [m^2]	HEAT FLOW IN [J/s]	MASS FLOW OUT [kg/s]:	
			POLYM	CHAR
TOP	1.000000e+000	3.924386e+004	0.000000e+000	0.000000e+000
BOTTOM	1.000000e+000	-3.219558e+003	0.000000e+000	0.000000e+000

FROM TOP [m]	TEMPERATURE [K]	CONCENTRATION [kg/m^3]:	
		POLYM	CHAR
1.000000e-005	5.673756e+002	9.999999e+002	3.269199e-006
3.050000e-004	5.257082e+002	1.000000e+003	5.382815e-008
6.050000e-004	5.071237e+002	1.000000e+003	1.280688e-008
9.050000e-004	5.014103e+002	1.000000e+003	9.923274e-009
1.205000e-003	5.001970e+002	1.000000e+003	9.590456e-009
1.505000e-003	5.000199e+002	1.000000e+003	9.555702e-009
1.805000e-003	5.000015e+002	1.000000e+003	9.552834e-009
2.105000e-003	5.000001e+002	1.000000e+003	9.552645e-009
2.405000e-003	5.000000e+002	1.000000e+003	9.552635e-009
2.705000e-003	5.000000e+002	1.000000e+003	9.552634e-009
3.005000e-003	5.000000e+002	1.000000e+003	9.552631e-009
3.305000e-003	4.999997e+002	1.000000e+003	9.552588e-009
3.605000e-003	4.999960e+002	1.000000e+003	9.551976e-009
3.905000e-003	4.999647e+002	1.000000e+003	9.545272e-009
4.205000e-003	4.997764e+002	1.000000e+003	9.490422e-009
4.505000e-003	4.990020e+002	1.000000e+003	9.169662e-009
4.805000e-003	4.968006e+002	1.000000e+003	7.889988e-009
4.985000e-003	4.944413e+002	1.000000e+003	6.200658e-009

Total thickness [m] = 5.000000e-003
Total mass [kg/m^2] = 5.000000e+000

Calculations are complete.
Total runtime: 0 minutes